

Network-based genetic monitoring of landscape fragmentation

Ohad Peled¹, Jaehee Kim², and Gili Greenbaum¹

¹*Department of Ecology, Evolution and Behavior, The Hebrew University of Jerusalem, Jerusalem, Israel*

²*Department of Computational Biology, Cornell University, Ithaca, NY, US*

Keywords: population genetics, network theory, fragmentation, conservation, genetic diversity

Classifications: Biological Sciences: Genetics, Population biology, Ecology, Biophysics and Computational Biology

Corresponding author: Gili Greenbaum (gil.G@mail.huji.ac.il)

Abstract

Habitat fragmentation is one of the most immediate and substantial threats to biodiversity, generating isolated populations with reduced genetic diversity. Genetic monitoring has become essential for detecting fragmentation and tracking its progress. However, the coherent interpretation of genetic monitoring data and understanding the genetic consequences of fragmentation require frameworks that accurately represent real-world complexity. Existing theoretical frameworks typically rely on simplified spatial structures and do not adequately capture the heterogeneous migration patterns of natural populations. Here, we integrate network theory and mathematical population genetics to develop a framework for studying the genetic consequences of fragmentation processes, explicitly accounting for heterogeneous connectivity and temporal dynamics. We apply this framework to examine how different fragmentation processes affect genetic measures commonly used in genetic monitoring. We find that different fragmentation scenarios produce substantially distinct trajectories in key genetic measures, sometimes exhibiting rapid transitional dynamics, suggesting that the interpretation of genetic monitoring data must be tailored to ecological contexts. Furthermore, fragmentation can cause deviations from classical theoretical expectations, such as the expected correlation between genetic and geographic distance (isolation-by-distance) or between genetic diversity and connectivity. Finally, we propose and demonstrate detectable early warning signals in genetic monitoring data that precede rapid transitional phases. Our framework thus provides a practical interpretation of genetic monitoring data, bridging the gap between idealized theoretical models and real-world connectivity dynamics.

Significance Statement

Landscape fragmentation threatens the persistence of species worldwide. Genetic monitoring is often used to track the genetic health of populations, but the relationship between real-world landscape connectivity and genetic measures remains difficult to model. Here, we integrate network theory with mathematical population genetics to develop a framework that addresses this challenge and enables interpretation of genetic measures along fragmentation processes in networks. We show that different fragmentation scenarios can generate qualitatively different genetic outcomes and violate classical population genetic principles. We also demonstrate that our approach can be used to identify early warning signals in genetic monitoring data before populations suffer significant declines in genetic health. Our framework bridges population genetic theory and conservation practice.

1 Introduction

2 Rapid human-induced environmental changes affect ecological and evolutionary processes, driving
3 biodiversity loss [1]. One of the main factors driving these changes is landscape fragmentation,
4 the partitioning of landscapes into small and weakly connected habitat patches [2]. Fragmentation
5 reduces connectivity among populations, constraining gene flow and dispersal of individuals [3],
6 which can negatively impact the health and viability of populations [4–6]. Landscape fragmen-
7 tation is expected to erode within-population genetic diversity and increase between-population
8 genetic differentiation due to reduced gene flow and increased genetic drift [7, 8]. Decreased genetic
9 diversity can, in turn, reduce population viability in the short term by increasing risks of inbreed-
10 ing depression [7, 9], while also limiting long-term evolutionary potential and adaptive capacity
11 in response to future environmental changes [10, 11]. Consequently, systematically and coher-
12 ently tracking fragmentation dynamics and their population-genetic consequences through genetic
13 monitoring remains a major goal in conservation biology.

14 Genetic monitoring of population genetic metrics over time is a cost-effective and direct approach
15 for tracking both the genetic impacts and the underlying ecological processes of fragmentation.
16 The alternative, tracking individual movement among habitat patches, is usually resource-intensive
17 and offers only an indirect proxy for the genetic and evolutionary consequences of fragmentation.
18 Consequently, genetic monitoring of wild populations is widely used to assess population health
19 and viability, landscape connectivity, and species responses to environmental disturbances [12–
20 14]. However, a major challenge in applying genetic monitoring to track fragmentation lies in the
21 interpretation of genetic measures in the context of the ecological process of migration.

22 Early theoretical work in population genetics established foundational frameworks for linking
23 genetic diversity and differentiation to migration under simplified assumptions about gene flow pat-
24 terns and spatial configurations [15–17]. For example, the island model assumes equal and constant
25 migration rates without explicit spatial arrangement [15], whereas the stepping-stone model incor-
26 porates homogeneous and symmetric migration between adjacent demes arranged on a regular lat-
27 tice with an additional long-range migration component [17]. These models provided fundamental
28 insights into how spatial connectivity shapes population genetic structure and introduced key con-
29 cepts such as isolation-by-distance, where genetic differentiation increases with geographic distance
30 [18], and the connectivity-diversity relationship, in which populations that are more connected are
31 expected to exhibit higher genetic diversity [19]. However, their simplified assumptions often limit
32 their practical applicability for genetic monitoring and evaluating fragmentation impacts [20]. For
33 example, one critical limitation of most existing modeling frameworks is their inability to capture
34 the temporal dynamics of fragmentation, where landscape degradation and connectivity loss occur
35 as heterogeneous, sequential processes shaped by the specific spatial and temporal characteristics
36 of anthropogenic or climatic drivers [21]. The lack of a modeling framework that integrates realistic
37 spatiotemporal patterns of connectivity and fragmentation thus restricts the practical application
38 of population genetic theory in conservation efforts and limits its utility for informing management

39 decisions.

40 A promising approach for incorporating realistic gene flow patterns into population genetic
41 theory is to represent connectivity between populations as a network—a mathematical construct
42 comprising nodes (habitat patches) connected by edges (connectivity) [22]. Population networks
43 can accommodate complex connectivity patterns beyond the scope of classical population genetics
44 models. Several methods have been developed to infer such networks from genetic data by quanti-
45 fying genetic differentiation between population pairs [23–25], with applications across a wide range
46 of taxa [23, 26–32]. These network-based approaches provide a rigorous framework for modeling
47 realistic fragmentation dynamics, enabling more coherent interpretations of genetic monitoring.

48 In this work, to bridge the gap between theory and practice, we develop a framework based
49 on population networks, integrating advances in population-genetic theory and network science to
50 investigate the spatiotemporal genetic consequences of landscape fragmentation. This framework
51 explicitly incorporates real-world complexities within a conceptually simple and tractable model.
52 We apply this framework to examine how different fragmentation scenarios affect genetic measures
53 and to assess how network structure impacts population resilience under connectivity loss. While
54 fragmentation is a multifaceted process involving multiple concurrent stressors (e.g., habitat loss,
55 reduced patch size, edge effects), our focus here is on connectivity loss (also termed fragmentation
56 *per se*; [5, 33]). Our approach enables improved interpretation of genetic monitoring data and
57 facilitates identification and measurement of fragmentation progression. Additionally, our modeling
58 framework can assist in predicting the genetic impacts of connectivity loss and evaluating the genetic
59 health of fragmented populations.

60 2 Results

61 To model the genetic consequences of fragmentation, we consider a metapopulation in which some
62 populations are connected by migration. For tractability, we assume equal and symmetric migra-
63 tion rates among all connected populations. Any such connectivity pattern can be represented as
64 a population network (Fig. 1a). To relate migration patterns to genetic measures, we employ the
65 approach developed by Alcala *et al.* [34], which consists of two transformations: (i) from migra-
66 tion matrices to pairwise coalescent-time matrices [35], and (ii) from coalescent-time matrices to
67 pairwise genetic differentiation measured by F_{ST} [36] (see *Methods* and Supplementary Information
68 Text). This procedure provides, for a given migration matrix, expected pairwise F_{ST} between all
69 population pairs, as well as genetic diversity measured by expected heterozygosity (H_e) for each
70 population (Fig. 1a). For simplicity, we further assume uniform population sizes and mutation
71 rates across all populations, allowing us to use an ‘unscaled’ heterozygosity measure (see *Methods*);
72 therefore, our H_e values should be interpreted only relatively, and values exceeding one are possible.

73 To simulate an ecologically plausible metapopulation, which is usually embedded in a geographic
74 landscape, we use a random geometric graph (RGG) model [37] as the initial network. In this model,
75 populations are more likely to be connected if they are geographically close to each other. We model

76 a fragmentation process by iteratively removing edges according to one of several predefined frag-
 77 mentation scenarios (Fig. 1b). After each edge removal, we recompute genetic measures, tracking
 78 their changes until all edges have been removed and the network has become fully fragmented into
 79 isolated populations. This modeling framework is highly flexible and enables the study of diverse
 80 connectivity patterns and fragmentation scenarios while providing rigorous analytical expectations
 81 for key genetic measures commonly used in genetic monitoring.

82 We consider eight fragmentation scenarios (Fig. 1b): (i) random fragmentation, representing
 83 global environmental changes (e.g., climate change); (ii) autocorrelated fragmentation, representing
 84 spatially correlated landscape disturbances (e.g., agricultural expansion); (iii) intrusive fragmenta-
 85 tion, representing the emergence of isolated habitats within the landscape; (iv) regressive fragmen-

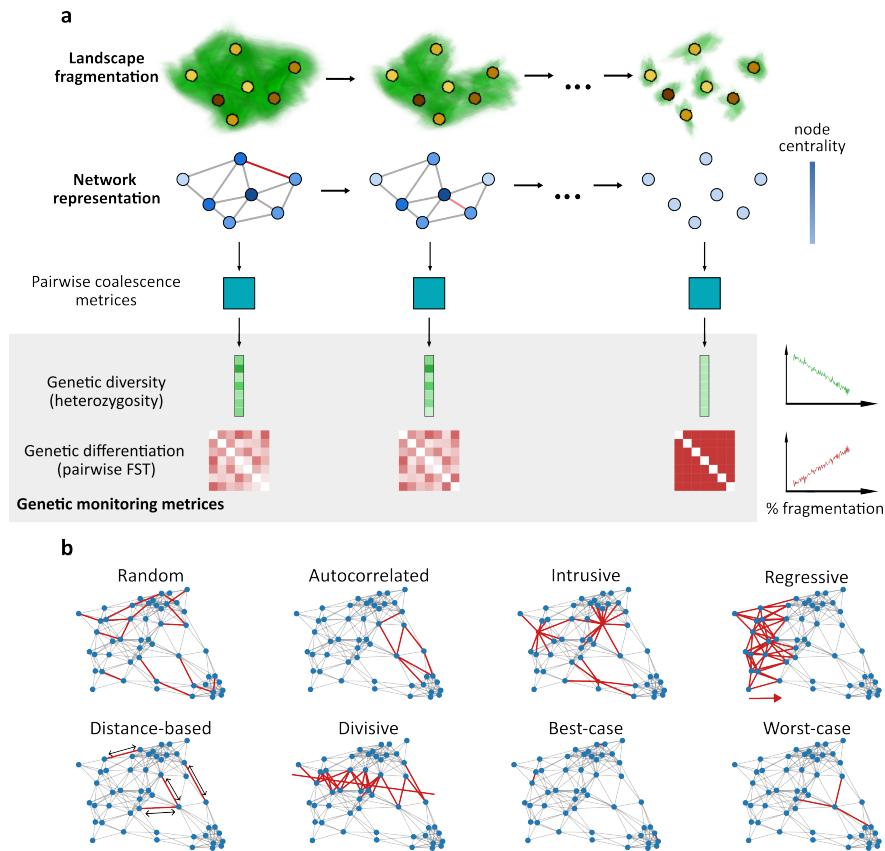


Figure 1: **Schematic representation of the network-based framework for modeling population genetic effects of fragmentation.** (a) Computation of genetic measures along fragmentation. In the top row, populations (yellow/brown patches) are embedded in a landscape (green) undergoing fragmentation. Below, the metapopulation is represented as a network with nodes (blue) denoting populations and edges representing migration between populations. Fragmentation is simulated by iteratively removing edges (red). A coalescence matrix is derived from each network, which enables the calculation of genetic diversity and differentiation at each fragmentation step (grey box). These metrics allow monitoring of population genetic changes over time (right side of the grey box). Color intensity of nodes represents network properties associated with genetic measures. (b) Modeling fragmentation processes. Illustrated are eight fragmentation scenarios applied to a single realization of a random geometric graph (RGG). Edges removed under each scenario are shown in red. Further details of each scenario are provided in the text.

86 tation, representing the expansion of a disturbance into a natural landscape (e.g., urban expansion);
 87 (v) distance-based fragmentation, representing reduced dispersal ability through a non-habitable
 88 matrix (e.g., disturbances hindering dispersal through the matrix, reducing dispersal distances);
 89 (vi) divisive fragmentation, representing linear destruction of connectivity (e.g., road or railway
 90 construction); (vii) best-case fragmentation, an idealized scenario that sequentially removes the
 91 least important edges, thus maximizing connectivity at each step; and (viii) worst-case fragmen-
 92 tation, similar to the best-case scenario, except the most important edge is removed at each step.
 93 The last two scenarios are theoretical constructs intended to establish upper and lower bounds for
 94 genetic measures rather than to depict realistic fragmentation processes. Detailed descriptions of
 95 each fragmentation scenario are provided in *Methods*.

96 2.1 Genetic monitoring measures strongly depend on the fragmentation sce- 97 nario

98 Across all fragmentation scenarios, we observe an increase in genetic differentiation and a decrease
 99 in genetic diversity as fragmentation progresses (Fig. 2). However, the rate and pattern of these
 100 changes vary substantially among scenarios. The slowest erosion of genetic diversity and the most
 101 gradual increase in genetic differentiation were observed under the best-case scenario (pink curve
 102 in Fig. 2), as expected. In contrast, the worst-case scenario exhibited the most rapid erosion of
 103 genetic diversity and the steepest increase in differentiation (grey curve in Fig. 2). Thus, these
 104 two theoretical extremes provide upper and lower bounds for the retention of genetic health in the
 105 metapopulation, against which other fragmentation scenarios can be compared.

106 In the random and autocorrelated scenarios, the loss of diversity and increase in differentiation
 107 are almost undetectable in the early stages of fragmentation but then become substantial at $\sim 60\%$
 108 fragmentation. This pattern is reflected in concave curves for genetic diversity and convex curves
 109 for differentiation (blue and orange curves in Fig. 2). The distance-based scenario (purple curve in

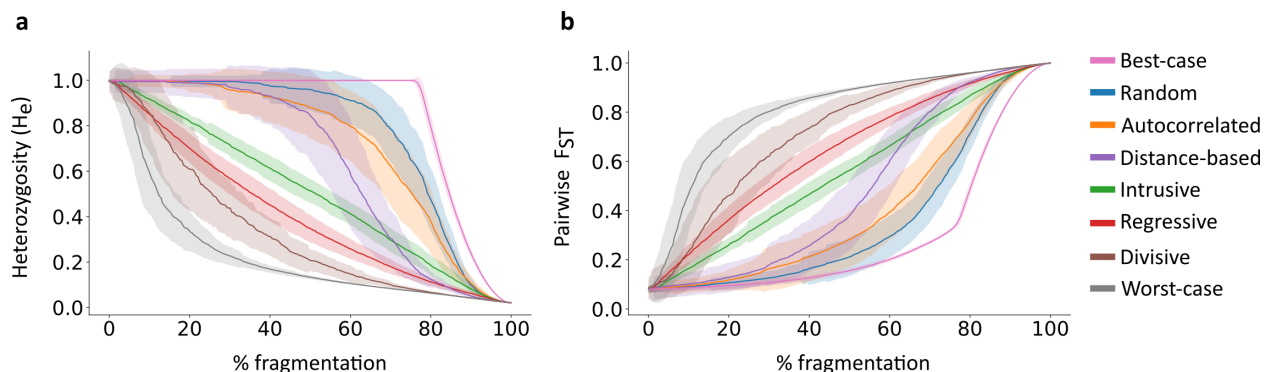


Figure 2: Changes in genetic measures along fragmentation under eight fragmentation scenarios.
 (a) Mean genetic diversity (H_e) across all populations along fragmentation. (b) Mean genetic differentiation (pairwise F_{ST}) among all population pairs. Lines denote means across 100 simulation replicates, with shaded regions indicating standard deviations. Fragmentation is measured as the fraction of edges removed from the initial network.

110 Fig. 2) shows a similar trend, but the loss of genetic diversity begins earlier in the fragmentation
111 process and progresses faster than in the random and autocorrelated scenarios. In contrast, in the
112 regressive and divisive scenarios, the curvature patterns are reversed: the genetic diversity curve is
113 convex, with rapid and substantial decreases in genetic diversity early in the fragmentation process,
114 and the genetic differentiation curve is concave, indicating earlier deterioration of metapopulation
115 genetic health compared to the other scenarios. For example, in the divisive scenario, a > 50%
116 change in genetic measures occurs already by 25% of the fragmentation process (brown curve
117 in Fig. 2). In the intrusive scenario, both genetic measures change approximately linearly as
118 fragmentation progresses (green curve in Fig. 2).

119 To understand the robustness of these patterns, we also examined how F_{ST} and H_e measures
120 change along fragmentation under different migration rates and initial network topologies (Figs. S1
121 and S2). Overall, the patterns remain similar across different migration rates, except at low mi-
122 gration rates, where the absolute values of F_{ST} are higher in the early stages of fragmentation
123 (Fig. S1b). Similarly, the results remained consistent when the initial network topologies were
124 generated using either the Erdős-Rényi model or a small-world network model instead of the RGG
125 model (Fig. S2). However, the differences among fragmentation scenarios were less pronounced in
126 these analyses, highlighting the importance of considering spatially explicit network models, such
127 as the RGG model.

128 Overall, our results demonstrate that, for a given level of connectivity loss, the risk of inbreeding
129 depression and the reductions in both evolutionary potential and between-population differentia-
130 tion strongly depend on the type of fragmentation process experienced by the metapopulation.
131 Therefore, the interpretation of genetic monitoring data must account for the context and drivers
132 of fragmentation. For example, a 10% decrease in H_e might reflect gradual connectivity decline un-
133 der intrusive fragmentation, whereas the same decrease under random fragmentation could indicate
134 dramatic habitat deterioration.

135 2.2 Relationship between heterozygosity and network components

136 When considering the distributions of the genetic measures rather than just their means, we observe
137 that H_e distributions remain largely unimodal throughout the fragmentation process, with a shift
138 towards $H_e = 0$ occurring as isolated nodes accumulate (Figs. 3a–c and S4a–e). Similarly, the
139 F_{ST} distributions exhibit increasing bimodality, with density accumulating at $F_{ST} = 1$ as more
140 nodes are separated into different components (Figs. 3d–f and S4f–j). Changes in the shape of
141 these distributions along fragmentation are also reflected in the variance of genetic diversity across
142 populations (Fig. 3g): the level of fragmentation that maximizes variance, as well as the maximum
143 variance value, differs among fragmentation scenarios. The increase in H_e variance can make
144 the detection of fragmentation—and genetic health in general—more challenging at intermediate
145 fragmentation levels because more populations will need to be sampled to correctly characterize
146 the genetic diversity state of the metapopulation.

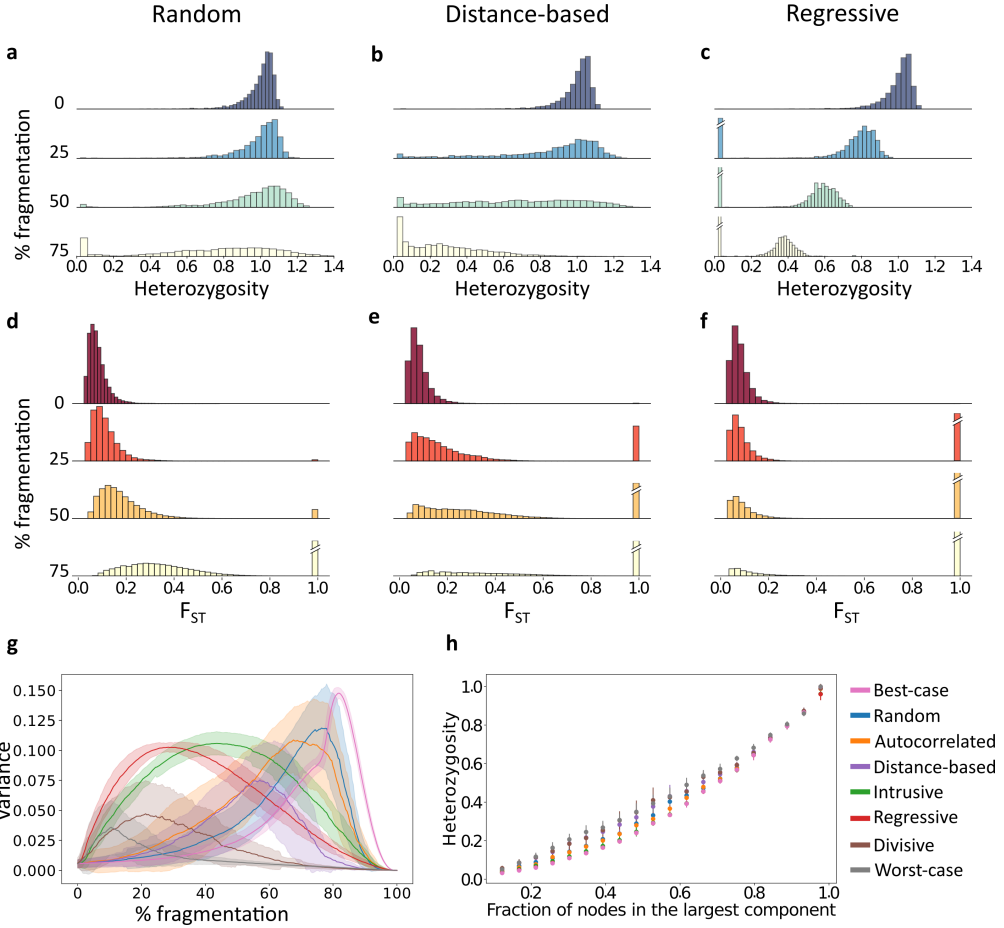


Figure 3: Changes in the distributions of genetic measures along fragmentation. Panels (a–f) show density distributions for three fragmentation scenarios: random, distance-based, and regressive (additional fragmentation scenarios are shown in Fig. S4). Four snapshots from the process are shown: 0%, 25%, 50%, and 75% fragmentation. Diagonal lines on bars indicate truncated values (for $H_e = 0$ or $F_{ST} = 1$). All distributions are pooled from 100 simulation replicates. (a–c) Distribution of expected heterozygosity (H_e) of populations. (d–f) Distribution of pairwise F_{ST} across all population pairs. (g) Change in the variance of H_e across all populations in the network. (h) Relationship between the fraction of nodes in the largest component and mean H_e across all populations in each network. For each scenario, dots denote the means across 100 simulation replicates, and lines denote the standard deviations.

As fragmentation progresses, network structure changes and populations begin to disconnect from the main component (Fig. S3). For example, the rapid deterioration in genetic health under the divisive scenario (brown in Fig. 2) can be attributed to the early emergence of medium and small network components, which reduce genetic diversity and increase between-component differentiation (Fig. S3f). To better understand the effect of component structure on genetic diversity, we tracked the size of the largest component throughout the fragmentation process (Fig. 3h). We observe a strong correlation between the size of the largest component and the mean H_e across populations in the network ($r = 0.97\text{--}0.98$ across scenarios, $p\text{-value} < 0.001$). This correlation is relatively consistent across different fragmentation scenarios, indicating that the size of the largest component is an important determinant of genetic diversity.

157 This result can be interpreted in relation to the theoretical relationship between effective pop-
158 ulation size and heterozygosity, $H_e = \frac{4N\mu}{1+4N\mu}$ [38]. Because we consider a small effective population
159 size relative to the mutation rate (i.e., $\theta = 4N\mu \ll 1$), we expect an approximately linear rela-
160 tionship of $H_e \approx 4N\mu$. The result in Fig. 3h is similar to what one would expect if we treated
161 each component as a well-mixed population. However, the relationship between H_e and component
162 size is sublinear, reflecting the fact that components are not well-mixed and should therefore be
163 represented with effective sizes smaller than their actual sizes.

164 2.3 Using network metrics in genetic monitoring

165 To better understand how tracking network characteristics can inform genetic monitoring, we eval-
166 uated the association between genetic measures and commonly used network metrics. We first
167 examined the relationship between a population’s genetic diversity and its centrality. There are
168 different ways to measure network centrality [39], each of which can be interpreted differently with
169 respect to population genetic processes [22]. Here, we evaluated two common metrics: degree
170 centrality (i.e., the number of edges incident to a node), which measures local centrality, and be-
171 tweenness centrality (i.e., the frequency with which a node lies on shortest paths between other
172 nodes), which measures global centrality. Under classical population genetics theory, populations
173 with higher connectivity should exhibit greater genetic diversity due to increased gene flow, leading
174 to higher H_e at migration-drift equilibrium [19]. Consistent with this expectation, analysis of the
175 initial (pre-fragmentation) networks showed a strong positive correlation between degree centrality
176 and H_e ($r = 0.71$ – 0.95 , Fig. 4a). However, because all populations had a relatively high H_e , this
177 relationship was nonlinear, exhibiting a saturating effect: while H_e increased with degree at low
178 connectivity, it plateaued for highly connected nodes (Fig. S5a). Hence, local connectivity increases
179 genetic diversity only up to a threshold, beyond which additional migration corridors do not sig-
180 nificantly contribute to maintaining genetic diversity. In contrast, the association between H_e and
181 betweenness centrality was weaker for nodes with low betweenness (Fig. S5b).

182 Throughout fragmentation, the correlation between H_e and degree centrality remains consis-
183 tently high for some scenarios but declines rapidly early in the fragmentation process under the
184 worst-case, divisive, and distance-based scenarios (Fig. 4a). This decline may result from network
185 partitioning into components of varying size in these fragmentation scenarios, where component
186 size has a stronger effect on H_e than does local connectivity. For example, a densely connected
187 population in a small component with few populations may have lower H_e than a sparsely con-
188 nected population in a larger component with many populations. Thus, component size, rather
189 than degree centrality, is a primary determinant of genetic diversity at these intermediate frag-
190 mentation stages. Interestingly, in these scenarios, the correlation later rebounds, converging to
191 levels similar to those of the other fragmentation scenarios. This suggests that once components
192 reach comparatively small sizes, within-component degree centrality once again becomes a strong
193 determinant of H_e .

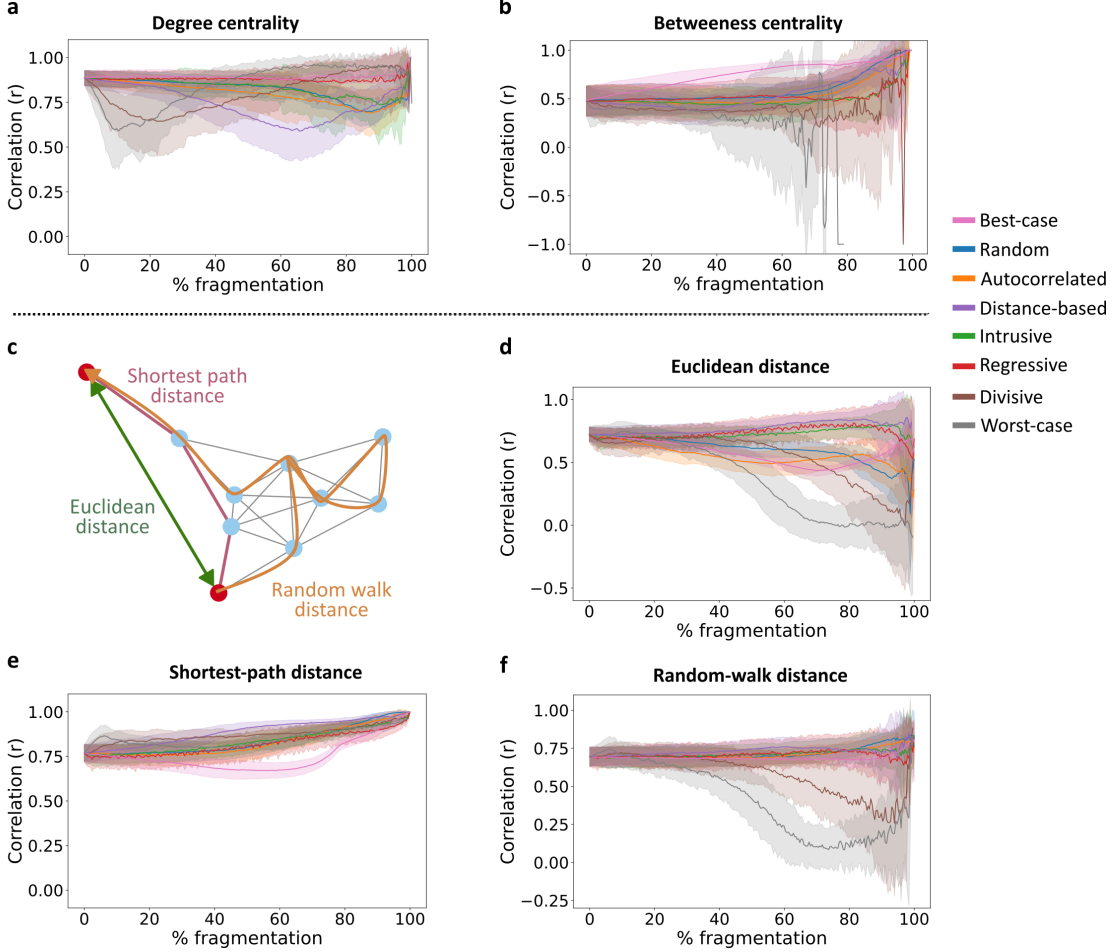


Figure 4: Correlation between population genetic measures and network metrics. The Pearson correlation coefficient r was computed between genetic diversity (H_e) and network centrality (panels a–b), or between genetic differentiation (F_{ST}) and distance metrics (panels c–f), for eight fragmentation scenarios. (a) Correlation between a population's H_e and its degree centrality (number of connected edges). (b) Correlation between a population's H_e and its betweenness centrality (global centrality metric). (c) Schematic illustration of three different distance metrics for a pair of populations (red nodes). (d) Correlation between the F_{ST} of a pair of populations and their Euclidean distance in the two-dimensional space in which the RGG network is embedded. (e) Correlation between the F_{ST} of a pair of populations and their shortest-path network distance. (f) Correlation between the F_{ST} of a pair of populations and their random-walk network distance.

The association between genetic diversity and betweenness centrality was generally weaker than that for degree centrality, with less variation among fragmentation scenarios (Fig. 4b). This suggests that populations do not necessarily need to occupy a key gene flow hub to maintain high genetic diversity, as has been observed in some systems [40]. One implication of this is that peripheral populations in large, well-connected networks can maintain genetic diversity comparable to that of central populations in smaller, less connected components.

Next, we examined the relationship between pairwise F_{ST} and three network distance metrics relevant for genetic monitoring (Fig. 4c): (i) Euclidean distance in the two-dimensional space

202 of the embedded RGG network, (ii) shortest-path distance (the minimum number of edges re-
203 quired to connect a pair of nodes), and (iii) random-walk distance (the expected number of edges
204 traversed in a random walk between two nodes). Euclidean distance represents the geographic
205 distance, whereas estimating the network distances requires knowledge of migration or movement
206 patterns in the metapopulation [22]. Prior to fragmentation, we observed strong correlations be-
207 tween F_{ST} and all three distance metrics ($r = 0.7\text{--}0.75$, Fig. 4d–f), indicating that geographically
208 distant populations are more genetically differentiated irrespective of how distance is measured.
209 This finding aligns with the isolation-by-distance expectation derived from stepping-stone [17] and
210 continuous-space [41] models, suggesting that such idealized models are a good approximation for
211 sufficiently well-connected networks [22]. However, as fragmentation progresses, these correlations
212 vary substantially both over the course of fragmentation and among scenarios (Fig. 4d–f).

213 For Euclidean distance, the correlation declines under most fragmentation scenarios, particularly
214 under the worst-case, divisive, best-case, and autocorrelated scenarios (Fig. 4d). Interestingly,
215 these processes differ substantially in their network structure during fragmentation, particularly
216 in the size of the largest connected component (Fig. S3), indicating that additional topological
217 properties are needed to account for the relationship between genetic differentiation and geographic
218 distance. In contrast, for shortest-path distance, the correlation consistently increases across most
219 processes we examined (the theoretical best-case scenario is the exception) and generally shows the
220 strongest association between F_{ST} and distance (Fig. 4e). This suggests that this network metric is
221 particularly suited for genetic monitoring, either as a non-genetic proxy for genetic differentiation or
222 as a proxy for connectivity from pairwise F_{ST} data. For the random-walk distance, the relationship
223 remains relatively stable throughout fragmentation for most scenarios, except for a decline in the
224 worst-case and divisive scenarios (Fig. 4f).

225 Overall, these analyses highlight that the topological properties of population networks can
226 inform the tracking of genetic diversity and differentiation patterns. However, relating genetic
227 measures to network properties such as components, centrality, or distance measures should, in
228 most cases, be done in the context of the fragmentation scenario. Classical population genetic
229 relationships—such as those between gene flow and diversity or distance and differentiation—are
230 useful for well-connected populations but may diverge from classical theory when fragmentation
231 processes shape the topology of metapopulation connectivity.

232 **2.4 Early warning signals in genetic monitoring**

233 The goal of genetic monitoring is to track the genetic health of populations and to infer under-
234 lying ecological processes. However, our findings suggest that inferring fragmentation solely from
235 genetic metrics can be challenging because substantial shifts in genetic measures often occur only
236 in the later stages of fragmentation under certain fragmentation scenarios. In such cases, once
237 genetic diversity declines and population differentiation increases, the transition is both rapid and
238 pronounced (Fig. 2). This transition can be considered a tipping-point phase, before which it is

difficult to detect ongoing fragmentation by tracking the means of H_e and F_{ST} . This raises the question: Can genetic monitoring data detect landscape fragmentation early enough—before the population transitions to a highly fragmented and diversity-depleted state? In other words, if we are tracking genetic measures in a metapopulation that is progressively undergoing fragmentation, can we use genetic data to provide an early warning signal prior to the tipping-point phase during which genetic diversity and differentiation dramatically change? To address this question, we evaluated whether early warning signals can be extracted from genetic diversity measures, borrowing methods from complex systems theory [42, 43]. Our analysis provides proof-of-concept for the potential to integrate early warning methodologies into genetic monitoring frameworks.

For this demonstrative analysis, we focused on the genetic diversity under the autocorrelated fragmentation scenario, where edges are removed in a spatially coordinated manner. We first considered a genetic monitoring scheme that tracks the H_e distributions of all populations throughout fragmentation (Fig. 5a). At each time step, we analyzed the distribution of H_e across populations and computed several summary statistics—standard deviation, skewness, and kurtosis—which have been found to be reliable early warning indicators in other disciplines [44, 45]. Another common statistic, lag-1 autocorrelation, was not used because it is intended to measure stability around a single equilibrium [44, 46], which did not hold in our simulations. As the metapopulation approaches the tipping-point phase, the theoretical expectation is that the standard deviation of the H_e distribution will increase, the skewness will shift toward the new state (in this case, asymmetry towards lower H_e values), and the kurtosis will increase due to an increased frequency of extreme values [43, 45]. To evaluate this, we computed these summary statistics throughout fragmentation (green curves in Fig. 5b–d) and examined whether they show substantial changes prior to the tipping-point phase (the sharp drop in the orange curves at $\sim 80\text{--}90\%$ fragmentation in Fig. 5b–d).

Some early warning signals prior to the tipping-point phase were clearly observable in our analyses (Fig. 5b–d). For example, the standard deviation of the distribution of H_e across the metapopulation increases steadily as fragmentation progresses, and substantial changes in this statistic are observable at the early stages of fragmentation even when changes in the mean are not yet detected (Fig. 5b). Thus, by tracking the standard deviation among populations over time, a noticeable change in this summary statistic could be identified and used as an early warning signal before the tipping-point phase. The mean skewness and kurtosis also showed early changes that can serve as early warning signals (Fig. 5c–d). However, the trajectories of skewness and kurtosis fluctuated over time and were noisier than the standard deviation, suggesting that they are less reliable as early warning indicators. This means that, while tracking the mean metapopulation H_e would not indicate that a rapid reduction in genetic health is approaching, monitoring higher moments could potentially provide an early indication of genetic deterioration.

We also considered a more limited monitoring scenario, where H_e is monitored for a single population (Fig. 5e). In this setting, a single population is tracked over time, and we evaluate the H_e distribution of 25% sliding temporal windows throughout fragmentation. As with the previous scenario, we tracked changes in the summary statistics of the distributions along fragmentation.

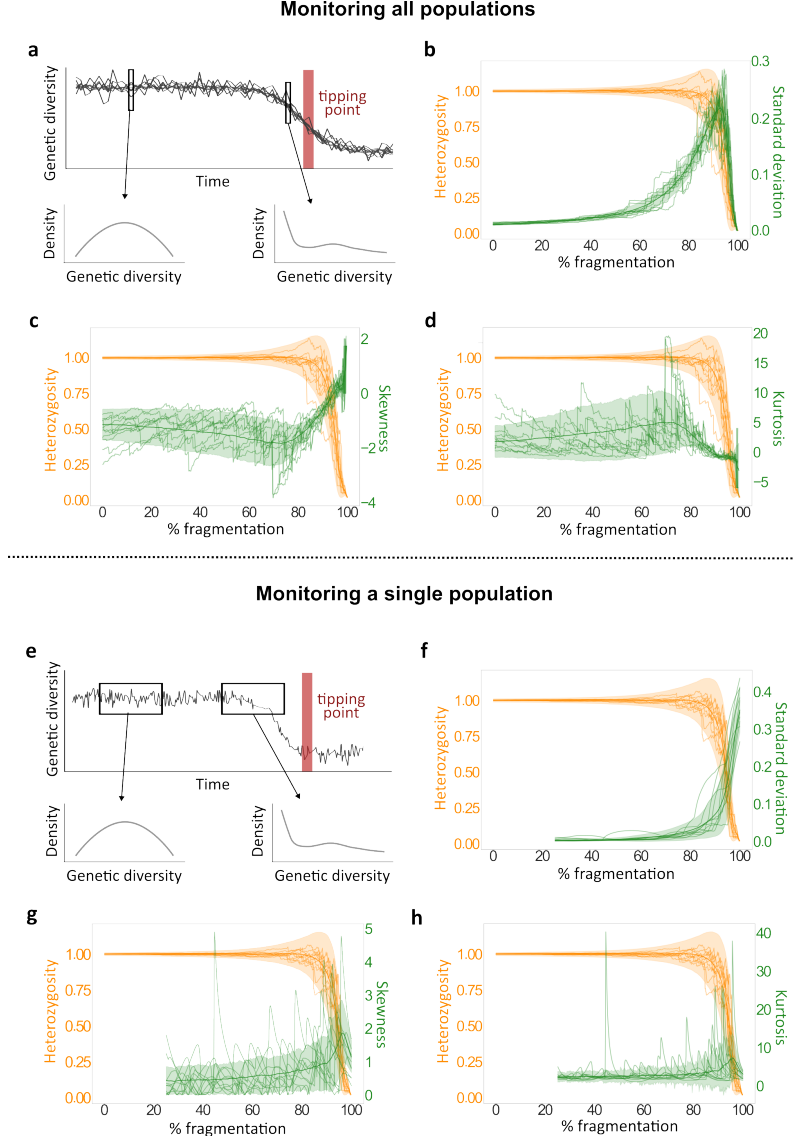


Figure 5: Early warning signals before tipping point in genetic monitoring. The analysis examines fragmentation under the autocorrelated scenario (Fig. 1b). (a) Schematic of the metapopulation-monitoring approach. At each time step, we analyze the H_e distribution of all connected populations in the network (largest component). The tipping-point phase, during which genetic diversity dramatically declines, is denoted in red. Genetic diversity distributions closer to the tipping-point phase may differ, with summary statistics potentially providing early warning. (b–d) Mean metapopulation heterozygosity (orange) and three early warning statistics (green: SD in (b), skewness in (c), and kurtosis in (d)) along fragmentation. Solid lines show the mean across 1000 simulation replicates, shaded areas show the standard deviation, and thin lines show ten individual replicates. (e) Schematic of the single-population monitoring approach. The H_e of a single population is tracked with a sliding window; the H_e distributions in each window are then analyzed. The tipping-point phase is shown in red. As above, the genetic diversity distributions in windows closer to the tipping-point phase may differ, with summary statistics potentially providing an early warning. (f–h) Mean metapopulation heterozygosity (orange) and three early warning statistics computed from 25% of the data per window (green: SD in (f), skewness in (g), and kurtosis in (h)). Solid lines show the mean across 1000 simulation replicates, shaded areas show the standard deviation, and thin lines show ten individual replicates.

278 Unlike the scenario that tracks the entire metapopulation, here we were not able to identify substantial
279 early warning signals (Fig. 5f–h). While the standard deviation did increase as fragmentation
280 progressed, the change was not substantial prior to the tipping-point phase (Fig. 5f). Although
281 no directional change in kurtosis was observed, skewness showed a moderate early increase, which
282 could potentially provide some early warning (Fig. 5g, h). Taken together, our analyses indicate
283 that under the simulation settings examined, cross-sectional monitoring of multiple populations
284 at each sampling occasion yields earlier and more reliable early warning signals than tracking a
285 single population through time, even when the latter is summarized over an extended temporal
286 window. The likely reason is that the cross-sectional snapshot includes multiple quasi-independent
287 observations per time step, whereas the sliding-window yields serially autocorrelated records.

288 3 Discussion

289 Habitat fragmentation is one of the most pressing threats to global biodiversity [2, 47], and genetic
290 monitoring could be instrumental in tracking and managing it. However, developing monitoring
291 and intervention strategies that take into account the real-world complexities of population struc-
292 ture remains a challenge [48, 49]. We present a framework that enables the modeling of habitat
293 fragmentation and its impacts on population genetic measures, thereby expanding the potential
294 scope of genetic monitoring. Using this framework, we model complex connectivity patterns and
295 simulate temporal dynamics and spatially heterogeneous fragmentation processes. We examined
296 the effects of different fragmentation scenarios on genetic measures and found that the same rate of
297 fragmentation can lead to markedly different patterns of genetic differentiation between populations
298 (F_{ST}) and levels of genetic diversity within populations (H_e). In this network-based perspective
299 of fragmentation, we also find that classical population genetic relationships, such as the asso-
300 ciation between F_{ST} and geographical distance or between gene flow and local genetic diversity,
301 may not always hold. Network topology metrics can help interpret these associations. Finally, we
302 demonstrate how genetic monitoring can potentially be used to detect early warning signals before
303 fragmentation triggers critical shifts in the genetic health of populations.

304 The population network framework presented here can be applied to study many ecological
305 processes that affect connectivity. Nonetheless, it is especially relevant in the context of genetic
306 monitoring because it can inform how genetic measures in populations change over time [50].
307 Human activity can induce fragmentation in different ways, but theoretical investigations of frag-
308 mentation dynamics and their potential consequences have thus far been limited [21, 51]. Our
309 results underscore the importance of considering the sequence of events leading to fragmentation
310 for accurate evaluation of its progression. While we observe steady rates of genetic changes that
311 are consistent with theory in some cases [52, 53], we also find scenarios in which genetic measures
312 change abruptly (Fig. 2).

313 An important factor in shaping the temporal change in genetic measures is the maximum num-
314 ber of connected populations in the network (i.e., the size of the largest component; Fig. 3h).

315 For example, scenarios in which a large component is maintained for a longer period (best-case,
316 random, autocorrelated; Fig. S3) maintain the genetic health of populations longer (Fig. 2). This
317 pattern holds even when populations within components are weakly or indirectly connected. From
318 a landscape management perspective, it implies that enhancing connectivity between network mod-
319 ules (i.e., clusters of connected populations) may be more beneficial for maintaining high levels of
320 genetic diversity than increasing direct connectivity within a weakly connected module. This result
321 is consistent with the expectation that larger populations (or metapopulations) will exhibit higher
322 genetic diversity due to increased gene flow and decreased genetic drift at the global scale [38].
323 However, increasing global connectivity can lead to homogenization of genetic pools and loss of
324 local adaptations [54, 55]. Therefore, considering the spatial scale at which connectivity between
325 populations is measured is crucial for accurately interpreting genetic monitoring outputs.

326 Populations and ecological systems facing environmental changes can undergo dramatic, unex-
327 pected, and often irreversible transitions. In the context of tracking biodiversity, several studies
328 have introduced the concept of fragmentation thresholds that lead to regime shifts in biodiversity
329 [56–58]. However, regime shifts in terms of genetic health and population-level metrics have re-
330 ceived far less attention and have been considered primarily in the context of adaptive evolution in
331 response to stress [59]. Consequently, genetic monitoring of populations is often reduced to qualita-
332 tive assessments. We demonstrated that genetic indicators may appear constant during substantial
333 periods of fragmentation, followed by rapid shifts in genetic metrics (e.g., random or autocorrelated
334 fragmentation in Fig. 2). This suggests that a standard interpretation of genetic monitoring—no
335 genetic change over time implies no underlying fragmentation process—can be misleading. As a
336 proof-of-concept, we showed that early warning signals may be detectable by tracking features of
337 the distributions of genetic monitoring data. This is particularly true if a large number of popula-
338 tions in the metapopulation are monitored. Although there is a substantial body of theoretical and
339 statistical literature on early warning signals [42, 43, 46, 60], to the best of our knowledge, no theo-
340 retical or empirical studies have explored the integration of these methods with population-genetic
341 data so far. Further investigation, applying a more comprehensive suite of early warning methods
342 (e.g., Kendall’s τ statistic, conditional heteroskedasticity) to empirical data, may shed additional
343 light on the effectiveness of this approach.

344 Patterns of spatial genetic structure have been extensively studied for almost a century, both
345 in theoretical population genetic models [17, 18, 35, 61] and in empirical studies of natural pop-
346 ulations [62–64]. One prevailing view is that spatial separation generates isolation-by-distance
347 patterns reflected in genetic differentiation measures [17, 18, 65]. However, we find that these pat-
348 terns may deviate from classical expectations depending on the underlying fragmentation scenario
349 and the distance metric used (Fig. 4c–f). Similarly, the relationship between genetic diversity and
350 connectivity [66–68], a key guideline in conservation practices [69], can also weaken during fragmen-
351 tation (Fig. 4a–b). These findings highlight the need to integrate complex spatial configurations of
352 populations and realistic descriptions of ecological processes into population genetic studies.

353 Although our framework is flexible and allows detailed spatial configurations, we assumed con-

stant population sizes and symmetric continuous migration rates, and we did not incorporate extinction-colonization dynamics. While our sensitivity analyses suggest that the way different fragmentation scenarios affect genetic measures is relatively general and not strongly affected by the initial network structure or migration rates, other ecological features may have important impacts. Our main goal, therefore, is to provide qualitative understanding of how genetic monitoring data should be interpreted, rather than to offer precise ways to represent realistic population dynamics. One important assumption in our model relates to the time required for a system to reach migration-drift equilibrium between fragmentation steps. When the rate of fragmentation is substantially faster than the rate of approach to equilibrium, our framework may not be appropriate. It has been suggested that genetic differentiation may respond more rapidly than heterozygosity to changes in migration [52] and reach equilibrium faster [70, 71]; therefore, in some cases, the framework may be suitable for tracking genetic differentiation but not genetic diversity.

As non-invasive population-genomic data become increasingly accessible, genetic monitoring is expected to emerge as a leading tool in conservation biology for assessing the health, ecology, and behavior of natural animal and plant populations. However, the gap between theoretical expectations and practical challenges in conservation biology currently limits our ability to accurately interpret genetic data and develop landscape-specific and species-specific conservation strategies. Our framework incorporates the real-world complexities of space and time and is readily interpretable in terms of genetic monitoring. Here, we explored an important aspect of fragmentation—the processes and patterns by which between-population connectivity is lost—but our framework can be readily expanded to investigate other anthropogenic effects, such as habitat loss (e.g., by simulating different node-removal processes) or the utility of interventions (e.g., prioritization of ecological corridors). Our network-based framework thus serves to narrow the gap between theoretical insights and the complex ecological realities of conservation biology.

4 Methods

All analyses were performed using Python 3.11.1, except where stated otherwise.

4.1 Computing genetic measures in population networks

To compute genetic measures for population networks, we employed the framework developed by Alcala *et al.* [34], which integrates the mathematical relationship between migration and coalescence times by Wilkinson-Herbots [35] with the relationship between coalescent times and F_{ST} by Slatkin [36]. Our method relies on transformations among three matrices: (i) the migration matrix describing the pairwise migration rates, (ii) the coalescence matrix describing the expected time to coalesce for two lineages within or between populations, and (iii) the F_{ST} matrix describing the pairwise genetic distance between populations. A full explanation of the derivations and computations is presented in the Supplementary Information Text.

We considered an idealized system of K populations of equal size, evolving under the neutral

Wright-Fisher model at migration-drift equilibrium [19]. Let m_{ij} denote the backward migration rate from population i to j , representing the probability that a lineage in i originated in j in the previous generation. We assumed symmetric migration ($m_{ij} = m_{ji}$ for all i and j) to ensure conservative migration [35], where total incoming and outgoing migration balance in each population: $\sum_{j \neq i} M_{ij} = \sum_{j \neq i} M_{ji}$. While conservative migration is a weaker assumption than symmetric migration, we imposed symmetric migration for tractability. Under these assumptions, the migration structure of the populations is represented as a symmetric, undirected network M of K nodes with zero-diagonal entries. For a pair of nodes i and j ($i \neq j$), the weight assigned to the edge is $M_{ij} = 4Nm_{ij}$, representing the expected number of migrants from i to j per generation, with N denoting the population size of each of the nodes. We simulated population networks with $K = 50$ nodes, where migration rates are uniform across all edges ($M_{ij} = 1$ in the main text, and alternative migration rates in Fig. S1).

4.2 Simulating fragmentation processes in population networks

Because natural populations are embedded in a geographic space, we used spatial network models [72], in which nodes correspond to populations with assigned geographic coordinates. We primarily used the random geometric graph (RGG) model [37], one of the simplest and most widely studied spatial network models, to generate the initial network in our simulations (see Fig. S2 for alternative network models). In this model, K populations are placed uniformly at random in a unit square in Euclidean space, and an edge is formed between two nodes if their Euclidean distance is below a fixed threshold d . The RGG model is particularly well-suited for representing migration in spatially structured populations because it captures the ecologically realistic constraint that migration occurs only between sufficiently proximate populations. The connectivity threshold for two-dimensional RGG networks (i.e., the value of d above which the network is almost surely connected) is $\sqrt{\frac{\log K}{\pi K}}$ [73], which equals $d = 0.16$ for $K = 50$. We therefore set $d = 0.30$, which consistently generates a connected network that is not too dense yet sufficiently above the threshold at which the network is close to being disconnected.

To model the fragmentation process, we sequentially remove edges from the initial network, one at a time, until no edges remain. We consider eight fragmentation scenarios (Fig. 1). (i) *Random fragmentation*. At each fragmentation step, an edge is removed uniformly at random, representing non-specific habitat deterioration, such as fragmentation induced by global climate change. (ii) *Autocorrelated fragmentation*. Initially, one random edge is removed. At each subsequent step, one edge is removed uniformly at random from the set of edges adjacent to the previously removed edge (i.e., edges sharing a node with the last removed edge). This process models spatially correlated landscape disturbances, such as urban or agricultural expansions. (iii) *Intrusive fragmentation*. A node is selected uniformly at random, and all its incident edges are removed in random order. Once these edges are removed, another node is chosen randomly, its incident edges are removed, and the process is repeated. This process generates isolated habitable “islands” within the landscape, representing, for example, the formation of micro-reserves—small, disconnected populations. (iv)

428 *Regressive fragmentation.* Edges are sorted by the minimum x-coordinate of their incident nodes in
429 the Euclidean plane and removed progressively from low to high x-coordinate values, starting with
430 the edge having the smallest x-coordinate. This process represents large-scale spatial disturbances
431 moving across the habitat, such as shifts in climate-change fronts. (v) *Distance-based fragmentation.*
432 At each step, the edge connecting the most distant populations in the underlying Euclidean space is
433 removed. This process represents a general environmental deterioration that impedes long-distance
434 dispersal among habitat patches. (vi) *Divisive fragmentation.* A line is drawn in the Euclidean plane
435 by connecting two points on different boundaries (either opposing or neighboring boundaries) of the
436 metric space (selected uniformly at random), effectively bisecting the habitat. All edges intersecting
437 this line are sequentially removed, starting with those having the smallest x-coordinate (as defined
438 in (iv)). This process models the introduction of linear barriers, such as roads or railways, into
439 the landscape. (vii) *Best-case fragmentation.* At each step, the edge with the lowest betweenness
440 centrality is removed. Betweenness centrality was computed with the NetworkX Python library.
441 Because such edges contribute minimally to network connectivity, removing them is expected to
442 have the least impact on genetic measures. Although this scenario is not realistic, it serves as an
443 upper benchmark for evaluating genetic measures at a given level of fragmentation. (viii) *Worst-
444 case fragmentation.* Similar to best-case fragmentation, but at each step, the edge with the highest
445 betweenness centrality is removed. This process provides a lower benchmark for genetic measures
446 at a given level of fragmentation.

447 These eight fragmentation processes do not exhaustively cover all possible scenarios, but rather
448 describe typical ecological and anthropogenic disturbance patterns relevant to genetic monitoring
449 [21, 74]. Because these processes are stochastic, we performed 100 independent replicates per
450 fragmentation type, randomizing the initial network configuration and the fragmentation sequence
451 in each replicate.

452 In each simulation replicate, we computed the changes in F_{ST} and H_e distributions in response
453 to fragmentation, assuming migration-drift equilibrium is reached between successive iterations
454 of edge removal. Each replicate generates a sequence of migration matrices M_0, \dots, M_x , with x
455 being the last fragmentation step. From these migration matrices, we computed corresponding
456 F_{ST} matrices F_0, \dots, F_x and H_e vectors H_0, \dots, H_x . These sequences reflect the changes in genetic
457 differentiation and genetic diversity throughout fragmentation. Using these sequences, we tracked
458 changes in the means (Fig. 2), sample variances (Fig. 3g) and distributions (Fig. 3a–f) of the genetic
459 measures along fragmentation.

460 We also evaluated changes in network structure throughout fragmentation by tracking for four
461 structural categories: (i) largest component, (ii) other components with > 3 populations (medium
462 components), (iii) components of 2–3 populations (pairs/triads), and (iv) isolated nodes. At each
463 time step, we computed the mean proportion of nodes in each category across simulation replicates.

464 To account for alternative patterns of gene flow in our initial network, and to evaluate their
465 effect on our main conclusions, we considered two additional models. (i) The Erdős–Rényi (ER)

random network [75], in which, for K populations, each pair of populations is connected by an edge with probability p . To generate a well- but not fully-connected initial network, we set $p = 0.1$ (125 edges in total). To allow spatially explicit analysis that can be compared to the RGG, we embedded this model in Euclidean space, with nodes placed uniformly at random. (ii) The small-world Watts–Strogatz (WS) network is constructed by connecting each population (node) to its k nearest neighbors in a ring topology, and then rewiring each edge with probability p to connect to a randomly chosen population (node), introducing long-range connections while preserving the total number of edges. The WS network can represent species with a life history of many short-distance dispersal events and an occasional long-distance dispersal event. We use a modified variant of this model to incorporate spatial characteristics to the network [76, 77]. We use the grid_graph function in the Python library NetworkX to generate a two-dimensional network with n nodes, setting $k = 4$ (4 neighbors for each node), and a re-wiring probability of p . This setting converges to the stepping stone model [17] for $p = 0$. For our simulations, we set $n = 49$ (a 7×7 matrix).

4.3 Correlations between genetic measures and node attributes

To investigate how network metrics influence genetic monitoring along fragmentation, we examined the relationship between genetic measures and network metrics. For each network at each fragmentation step, we computed two node centrality measures, degree centrality (number of incident edges for the focal node) and betweenness centrality (how often a node lies on the shortest paths between other pairs of nodes), for all nodes in the network. We then computed the Pearson correlation coefficient (r) between node's H_e and their centrality score, at each fragmentation step and for each centrality measure (we excluded isolated nodes, for which centrality is undefined). Then, we computed the mean r and its SD for each fragmentation step across the simulation replicates, for each one of the centrality metrics and each fragmentation scenario. We only show significant correlation results ($p < 0.05$) with data from 5 or more replicates.

Similarly, we evaluated the relationships between network distance metrics and pairwise F_{ST} . We computed the distance between all pairs of nodes in each fragmentation step using three distance metrics: (i) Euclidean distance, the standard geometric measure in the embedded metric space, analogous to the typical geographic distances among populations; (ii) shortest-path distance [78], calculated as the minimum number of edges needed to traverse from one node to another, reflecting topology-aware movement; (iii) random-walk distance [79], defined as the mean number of edges a random walker requires to travel from one node to another, which is suitable for movement that is unaware of the network topology or a non-targeted movement [22]. Random-walk distance was estimated using 50 random-walk iterations per pairwise comparison. The correlations were calculated only within connected components of size > 3 , and pairs of nodes in disconnected components were excluded from correlation calculations (these pairs have $F_{ST} = 1$ and are infinitely distant from each other for shortest-path and random walk distance). We computed the Pearson correlation coefficient (r) between the F_{ST} of all node pairs and their distance score, at each fragmentation step and for each distance metric. We used the mantel python library to perform

504 a Mantel test and calculate a corresponding p-value with 999 permutations. For networks with
505 multiple components, and hence multiple r and p -values, we calculated the weighted mean r and
506 p based on the component size. We then computed the mean r and its SD for each fragmentation
507 step across the simulation replicates, for each one of the distance metrics and each fragmentation
508 scenario. We only show significant correlation results ($p < 0.05$) with data from 5 or more replicates.

509 4.4 Detecting early warning signals before population collapse

510 To identify early warning signals, we computed several summary statistics of the genetic diversity
511 (H_e) distributions that are commonly used as early warning signals: standard deviation, skewness,
512 and kurtosis. As the process approaches the tipping-point phase, the theoretical expectation is
513 that the standard deviation of the H_e distribution will increase, the skewness will shift toward
514 lower H_e values (higher asymmetry), and increased frequency of extreme values will lead to higher
515 kurtosis [43, 45]. We did not use the lag-1 autocorrelation, although it is often used metric to
516 measure the return rate to equilibrium after a perturbation [44], because this statistic it is designed
517 to measure stability around a single equilibrium [44, 46], while our framework considers a series of
518 fragmentation events between each the system arrives at migration-drift equilibrium.

519 For this analysis, we focused on autocorrelated fragmentation (Fig. 2b). We used a more
520 connected initial network than used in previous analyses, an RGG with $d = 0.6$, to capture a
521 substantial period that is far from the tipping-point phase. We ran 1000 simulations replicates and
522 we considered two monitoring scenarios: (i) *entire metapopulation monitoring*, where we analyze
523 the H_e distribution across all populations in the network at each step, and (ii) *single population*
524 *monitoring*, focusing on the H_e of the final nodes to become isolated. In the latter case, we used
525 the `generic_ews` function from the R package `earlywarnings` to apply a sliding window approach
526 over time, with window size of 25% and default parameters without detrending or preprocessing
527 the data.

528 Data, Materials, and Software Availability

529 All code is available in the GitHub repository at <https://github.com/Greenbaum-Lab/fragmentation.git>

531 Acknowledgments

532 We thank Keith Harris and Eyal Halutz for their input and assistance in the analysis. The research
533 was funded by the Binational Science Foundation (BSF) Grant No. 2021244. OP was supported
534 by fellowships from the Israel Ministry of Environmental Protection and from the Minerva Center
535 for the study of Population Fragmentation (MCPF).

536 **Author contributions**

537 Conceptualization, OP, GG, and JK; Study design, OP, GG, and JK; Coding, OP; Analysis, OP;
538 Writing of Original Draft, OP; Review & Editing, OP, GG, and JK; Funding Acquisition, GG and
539 JK; Supervision, GG and JK.

540 **Competing interests**

541 The authors declare no competing interest.

542 **References**

- 543 1. Jaureguiberry, P. *et al.* The direct drivers of recent global anthropogenic biodiversity loss.
544 *Science Advances* **8**, eabm9982 (2022).
- 545 2. Haddad, N. *et al.* Habitat fragmentation and its lasting impact on Earth's ecosystems. *Science*
546 *Advances* **1** (2015).
- 547 3. Van Dyck, H. & Baguette, M. Dispersal behaviour in fragmented landscapes: routine or special
548 movements? *Basic and Applied Ecology* **6**, 535–545 (2005).
- 549 4. Fischer, J. & Lindenmayer, D. B. Landscape modification and habitat fragmentation: a syn-
550 thesis. *Global Ecology and Biogeography* **16**, 265–280 (2007).
- 551 5. Fahrig, L. Effects of habitat fragmentation on biodiversity. *Annual Review of Ecology, Evolu-*
552 *tion, and Systematics* **34**, 487–515 (2003).
- 553 6. Aguilar, R. *et al.* Habitat fragmentation reduces plant progeny quality: a global synthesis.
554 *Ecology Letters* **22**, 1163–1173 (2019).
- 555 7. Reed, D. H. & Frankham, R. Correlation between fitness and genetic diversity. *Conservation*
556 *Biology* **17**, 230–237 (2003).
- 557 8. Lowe, A., Boshier, D., Ward, M., Bacles, C. & Navarro, C. Genetic resource impacts of habitat
558 loss and degradation; reconciling empirical evidence and predicted theory for neotropical trees.
559 *Heredity* **95**, 255–273 (2005).
- 560 9. Charlesworth, D. & Willis, J. H. The genetics of inbreeding depression. *Nature Reviews Ge-*
561 *netics* **10**, 783–796 (2009).
- 562 10. Jump, A. S., Marchant, R. & Peñuelas, J. Environmental change and the option value of
563 genetic diversity. *Trends in Plant Science* **14**, 51–58 (2009).
- 564 11. Manel, S. & Holderegger, R. Ten years of landscape genetics. *Trends in Ecology & Evolution*
565 **28**, 614–621 (2013).

- 566 12. Siol, M., Bonnin, I., Olivieri, I., Prosperi, J. & Ronfort, J. Effective population size associated
567 with self-fertilization: lessons from temporal changes in allele frequencies in the selfing annual
568 *Medicago truncatula*. *Journal of Evolutionary Biology* **20**, 2349–2360 (2007).
- 569 13. Kendall, K. C. *et al.* Demography and genetic structure of a recovering grizzly bear population.
570 *The Journal of Wildlife Management* **73**, 3–16 (2009).
- 571 14. Hauser, L., Adcock, G. J., Smith, P. J., Bernal Ramírez, J. H. & Carvalho, G. R. Loss of
572 microsatellite diversity and low effective population size in an overexploited population of
573 New Zealand snapper (*Pagrus auratus*). *Proceedings of the National Academy of Sciences* **99**,
574 11742–11747 (2002).
- 575 15. Wright, S. *The roles of mutation, inbreeding, crossbreeding and selection in evolution* in *Pro-*
576 *ceedings of the Sixth International Congress of Genetics* **1** (1932), 356–366.
- 577 16. Levene, H. Genetic equilibrium when more than one ecological niche is available. *The American*
578 *Naturalist* **87**, 331–333 (1953).
- 579 17. Kimura, M. & Weiss, G. H. The stepping stone model of population structure and the decrease
580 of genetic correlation with distance. *Genetics* **49**, 561 (1964).
- 581 18. Wright, S. Isolation by distance. *Genetics* **28**, 114 (1943).
- 582 19. Wright, S. Evolution in Mendelian populations. *Genetics* **16**, 97 (1931).
- 583 20. Sexton, J. P., Hangartner, S. B. & Hoffmann, A. A. Genetic isolation by environment or
584 distance: which pattern of gene flow is most common? *Evolution* **68**, 1–15 (2014).
- 585 21. Harris, L. D. & Silva-Lopez, G. *Forest fragmentation and the conservation of biological diver-*
586 *sity in Conservation biology: The theory and practice of nature conservation preservation and*
587 *management* (Springer, 1992), 197–237.
- 588 22. Greenbaum, G. & Fefferman, N. H. Application of network methods for understanding evolu-
589 *tionary dynamics in discrete habitats. Molecular Ecology* **26**, 2850–2863 (2017).
- 590 23. Dyer, R. J. & Nason, J. D. Population graphs: the graph theoretic shape of genetic structure.
591 *Molecular Ecology* **13**, 1713–1727 (2004).
- 592 24. Rozenfeld, A. F. *et al.* Network analysis identifies weak and strong links in a metapopulation
593 system. *Proceedings of the National Academy of Sciences* **105**, 18824–18829 (2008).
- 594 25. Dyer, R. J., Nason, J. D. & Garrick, R. C. Landscape modelling of gene flow: improved power
595 using conditional genetic distance derived from the topology of population networks. *Molecular*
596 *Ecology* **19**, 3746–3759 (2010).
- 597 26. Ball, M. C., Finnegan, L., Manseau, M. & Wilson, P. Integrating multiple analytical ap-
598 proaches to spatially delineate and characterize genetic population structure: an application
599 to boreal caribou (*Rangifer tarandus caribou*) in central Canada. *Conservation Genetics* **11**,
600 2131–2143 (2010).

- 601 27. Munwes, I. *et al.* The change in genetic diversity down the core-edge gradient in the eastern
602 spadefoot toad (*Pelobates syriacus*). *Molecular Ecology* **19**, 2675–2689 (2010).
- 603 28. Fitzpatrick, J., Carlon, D., Lippe, C. & Robertson, D. R. The West Pacific diversity hotspot as
604 a source or sink for new species? Population genetic insights from the Indo-Pacific parrotfish
605 *Scarus rubroviolaceus*. *Molecular Ecology* **20**, 219–234 (2011).
- 606 29. Garraway, C. J., Bowman, J. & Wilson, P. J. Using a genetic network to parameterize a
607 landscape resistance surface for fishers, *Martes pennanti*. *Molecular Ecology* **20**, 3978–3988
608 (2011).
- 609 30. Paschou, P. *et al.* Maritime route of colonization of Europe. *Proceedings of the National
610 Academy of Sciences* **111**, 9211–9216 (2014).
- 611 31. Werth, S. & Scheidegger, C. Gene flow within and between catchments in the threatened
612 riparian plant *Myricaria germanica*. *PLOS One* **9**, e99400 (2014).
- 613 32. Windmaißer, T., Kattari, S., Heubl, G. & Reisch, C. Glacial refugia and postglacial expansion
614 of the alpine–prealpine plant species *Polygala chamaebuxus*. *Ecology and Evolution* **6**, 7809–
615 7819 (2016).
- 616 33. Fahrig, L. Ecological responses to habitat fragmentation per se. *Annual Review of Ecology,
617 Evolution, and Systematics* **48**, 1–23 (2017).
- 618 34. Alcala, N., Goldberg, A., Ramakrishnan, U. & Rosenberg, N. A. Coalescent theory of migration
619 network motifs. *Molecular Biology and Evolution* **36**, 2358–2374 (2019).
- 620 35. Wilkinson-Herbots, H. M. Genealogy and subpopulation differentiation under various models
621 of population structure. *Journal of Mathematical Biology* **37**, 535–585 (1998).
- 622 36. Slatkin, M. Inbreeding coefficients and coalescence times. *Genetics Research* **58**, 167–175
623 (1991).
- 624 37. Dall, J. & Christensen, M. Random geometric graphs. *Physical Review E* **66**, 016121 (2002).
- 625 38. Kimura, M. Theoretical foundation of population genetics at the molecular level. *Theoretical
626 Population Biology* **2**, 174–208 (1971).
- 627 39. Rodrigues, F. A. *Network centrality: an introduction in A mathematical modeling approach
628 from nonlinear dynamics to complex systems* (Springer, 2018), 177–196.
- 629 40. Rodger, Y. S., Greenbaum, G., Silver, M., Bar-David, S. & Winters, G. Detecting hierarchical
630 levels of connectivity in a population of *Acacia tortilis* at the northern edge of the species'
631 global distribution: Combining classical population genetics and network analyses. *PLOS One*
632 **13**, e0194901 (2018).
- 633 41. Malécot, G. *Quelques schémas probabilistes sur la variabilité des populations naturelles* in
634 *Annales de l'Université de Lyon A* **13** (1950), 37–60.
- 635 42. Scheffer, M., Carpenter, S., Foley, J. A., Folke, C. & Walker, B. Catastrophic shifts in ecosystems.
636 *Nature* **413**, 591–596 (2001).

- 637 43. Scheffer, M. *et al.* Early-warning signals for critical transitions. *Nature* **461**, 53–59 (2009).
- 638 44. Dakos, V. *et al.* Methods for detecting early warnings of critical transitions in time series
639 illustrated using simulated ecological data. *PLOS One* **7**, e41010 (2012).
- 640 45. Guttal, V. & Jayaprakash, C. Changing skewness: an early warning signal of regime shifts in
641 ecosystems. *Ecology Letters* **11**, 450–460 (2008).
- 642 46. Veraart, A. J. *et al.* Recovery rates reflect distance to a tipping point in a living system.
643 *Nature* **481**, 357–359 (2012).
- 644 47. Hanski, I. Habitat fragmentation and species richness. *Journal of Biogeography* **42** (2015).
- 645 48. Watson, D. *et al.* Monitoring ecological consequences of efforts to restore landscape-scale
646 connectivity. *Biological Conservation* **206**, 201–209 (2017).
- 647 49. Frankham, R. Challenges and opportunities of genetic approaches to biological conservation.
648 *Biological Conservation* **143**, 1919–1927 (2010).
- 649 50. Schwartz, M. K., Luikart, G. & Waples, R. S. Genetic monitoring as a promising tool for
650 conservation and management. *Trends in Ecology & Evolution* **22**, 25–33 (2007).
- 651 51. Riitters, K., Wickham, J., O'Neill, R., Jones, B. & Smith, E. Global-scale patterns of forest
652 fragmentation. *Conservation Ecology* **4** (2000).
- 653 52. Keyghobadi, N., Roland, J., Matter, S. & Strobeck, C. Among- and within-patch compo-
654 nents of genetic diversity respond at different rates to habitat fragmentation: an empirical
655 demonstration. *Proceedings of the Royal Society B: Biological Sciences* **272**, 553–560 (2005).
- 656 53. Allendorf, F. W. Genetic drift and the loss of alleles versus heterozygosity. *Zoo Biology* **5**,
657 181–190 (1986).
- 658 54. Templeton, A. R. *Population genetics and microevolutionary theory* (John Wiley & Sons,
659 2021).
- 660 55. Templeton, A. R. Mechanisms of speciation—a population genetic approach. *Annual Review*
661 *of Ecology and Systematics*, 23–48 (1981).
- 662 56. Andren, H. Effects of habitat fragmentation on birds and mammals in landscapes with different
663 proportions of suitable habitat: a review. *Oikos*, 355–366 (1994).
- 664 57. Andren, H. Population responses to habitat fragmentation: statistical power and the random
665 sample hypothesis. *Oikos*, 235–242 (1996).
- 666 58. Pardini, R., Bueno, A., Gardner, T., Prado, P. & Metzger, J. Beyond the fragmentation
667 threshold hypothesis: Regime shifts in biodiversity across fragmented landscapes. *PLOS One*
668 **5** (2010).
- 669 59. Hoffmann, A. A. & Willi, Y. Detecting genetic responses to environmental change. *Nature*
670 *Reviews Genetics* **9**, 421–432 (2008).

- 671 60. Dakos, V. *et al.* Slowing down as an early warning signal for abrupt climate change. *Proceedings*
672 *of the National Academy of Sciences* **105**, 14308–14312 (2008).
- 673 61. Epperson, B. K. *Geographical genetics (MPB-38)* (Princeton University Press, 2003).
- 674 62. Crispo, E. & Hendry, A. Does time since colonization influence isolation by distance? A meta-
675 analysis. *Conservation Genetics* **6**, 665–682 (2005).
- 676 63. Jenkins, D. G. *et al.* A meta-analysis of isolation by distance: relic or reference standard for
677 landscape genetics? *Ecography* **33**, 315–320 (2010).
- 678 64. Storfer, A., Murphy, M. A., Spear, S. F., Holderegger, R. & Waits, L. P. Landscape genetics:
679 where are we now? *Molecular Ecology* **19**, 3496–3514 (2010).
- 680 65. Ramachandran, S. *et al.* Support from the relationship of genetic and geographic distance in
681 human populations for a serial founder effect originating in Africa. *Proceedings of the National*
682 *Academy of Sciences* **102**, 15942–15947 (2005).
- 683 66. Gómez-Fernández, A., Alcocer, I. & Matesanz, S. Does higher connectivity lead to higher ge-
684 netic diversity? Effects of habitat fragmentation on genetic variation and population structure
685 in a gypsophile. *Conservation Genetics* **17**, 631–641 (2016).
- 686 67. Wasserman, T. N., Cushman, S. A., Littell, J. S., Shirk, A. J. & Landguth, E. L. Population
687 connectivity and genetic diversity of American marten (*Martes americana*) in the United
688 States northern Rocky Mountains in a climate change context. *Conservation Genetics* **14**,
689 529–541 (2013).
- 690 68. Jangjoo, M., Matter, S. F., Roland, J. & Keyghobadi, N. Connectivity rescues genetic diversity
691 after a demographic bottleneck in a butterfly population network. *Proceedings of the National*
692 *Academy of Sciences* **113**, 10914–10919 (2016).
- 693 69. Kool, J. T., Moilanen, A. & Treml, E. A. Population connectivity: recent advances and new
694 perspectives. *Landscape Ecology* **28**, 165–185 (2013).
- 695 70. Crow, J. F. & Aoki, K. Group selection for a polygenic behavioral trait: estimating the degree
696 of population subdivision. *Proceedings of the National Academy of Sciences* **81**, 6073–6077
697 (1984).
- 698 71. Varvio, S.-L., Chakraborty, R. & Nei, M. Genetic variation in subdivided populations and
699 conservation genetics. *Heredity* **57**, 189–198 (1986).
- 700 72. Barthélémy, M. Spatial networks. *Physics Reports* **499**, 1–101 (2011).
- 701 73. Penrose, M. *Random geometric graphs* (OUP Oxford, 2003).
- 702 74. Marsh, L. K. *The nature of fragmentation in Primates in fragments: Ecology and conservation*
703 (Springer, 2003), 1–10.
- 704 75. Erdős, P., Rényi, A., *et al.* On the evolution of random graphs. *Publications of the Mathemat-
705 ical Institute of the Hungarian Academy of Sciences* **5**, 17–60 (1960).

- 706 76. Sen, P., Banerjee, K. & Biswas, T. Phase transitions in a network with a range-dependent
707 connection probability. *Physical Review E* **66**, 037102 (2002).
- 708 77. Newman, M. E. & Watts, D. J. Scaling and percolation in the small-world network model.
709 *Physical Review E* **60**, 7332 (1999).
- 710 78. Eppstein, D. Finding the k shortest paths. *SIAM Journal on Computing* **28**, 652–673 (1998).
- 711 79. Noh, J. D. & Rieger, H. Random walks on complex networks. *Physical Review Letters* **92**,
712 118701 (2004).